Evidence of jovian active longitude: 2. A parametric study.

Patrick H. M. Galopeau, Mohammed Y. Boudjada, Helmut O. Rucker

Evidence of Jovian active longitude: 2. A parametric study

Patrick H. M. Galopeau,[1] Mohammed Y. Boudjada,[2] and Helmut O. Rucker[2]

Received 13 June 2006; revised 23 October 2006; accepted 17 November 2006; published 24 April 2007.

[1] In a previous work, we developed a model allowing a theoretical location of the Io-controlled decameter radio sources (Io-A, Io-B, Io-C, and Io-D) in the central meridian longitude-Io phase diagram. This model considers the cyclotron maser instability to be at the origin of most auroral planetary radio emissions. We derive the efficiency of this theoretical mechanism at the footprint of the Io flux tube during a complete revolution of the satellite around Jupiter, and we show that some longitudes in the northern and southern hemispheres favor the radio decameter emission and lead to a probability of higher occurrence. In order to make the calculation easier, we suppose that electrons are accelerated in the neighborhood of Io and follow an adiabatic motion along magnetic field lines carried by the satellite. We also assume that the source of free energy needed by the cyclotron maser instability to amplify the waves derives from a loss cone distribution function built up by electrons which have disappeared in Jupiter's ionosphere. We study the effect of several parameters on the theoretical location of the sources in the central meridian longitude-Io phase diagram, in particular the Jovicentric declination of the Earth and the frequency of emission.

Citation: Galopeau, P. H. M., M. Y. Boudjada, and H. O. Rucker (2007), Evidence of Jovian active longitude: 2. A parametric study, *J. Geophys. Res.*, *112*, A04211, doi:10.1029/2006JA011911.

1. Introduction

[2] Long-term ground observations of the Jovian decameter radio emission (hereafter DAM) show that the occurrence probability of the radiation depends on two essential parameters: the central meridian longitude (CML, System III) which is linked to the rotating magnetic field and the orbital phase of the satellite Io [*Bigg*, 1964]. The CML-Io phase diagram, which displays the occurrence of the emission as a function of the CML and the Io phase, reveals several zones of enhanced occurrence probability which have been named Io-controlled sources: Io-A, Io-B, Io-C, and Io-D [*Carr et al.*, 1983]. In the following we perform a parametric study which extends the results of a recent paper [*Galopeau et al.*, 2004] (hereinafter referred to as paper 1), which showed theoretical evidence of the existence of a Jovian active longitude and the dependence of the source occurrence areas on the Jovicentric declination of the Earth along with the observation frequency conditions.

1.1. Jovian Active Longitude

[3] The originality of the theoretical approach we developed in paper 1 lies in the fact that, for the first time, we explain why the so-called Io-controlled sources occur at some specific longitudes, i.e., from 90° to 200° CML, and from 210° to 270° CML. Within the framework of the cyclotron maser instability, which is supposed to be the mechanism at the origin of most nonthermal planetary radio emissions, we showed in paper 1 that some longitudes in the northern and southern Jovian hemispheres favor the radio decameter emission and induce a higher occurrence probability. We also computed the efficiency of this theoretical mechanism at the footprint of the Io flux tube during a complete revolution of this satellite around Jupiter.

1.2. Latitudinal Beaming of Jovian Decametric Emissions

[4] Ground-based studies of Jovian decametric (DAM) radiations performed over the past fifty years reveal distinct variations in the DAM morphology. These changes depend on the declination of the Earth with respect to the Jovigraphic equatorial plane, which is usually called the Jovicentric declination of the Earth (hereafter D_E) and ranges between $-3.3°$ and $+3.3°$ over Jupiter's 11.9-year solar revolution period. Therefore both the System III central meridian longitude and the relative occurrence probability for decametric activity are observed to vary significantly as D_E changes over this interval [see *Carr et al.*, 1983, and references therein]. Several studies have estimated the variation of the Jovian DAM activity versus the Jovicentric declination. For the Io-controlled emissions, Io-A, Io-B and Io-C, the main investigations are based on observations recorded by three different radio telescopes. They are founded on studies by *Lecacheux* [1974] for the Boulder observations, *Thieman et al.* [1975] for the Florida station, and *Boudjada and Leblanc* [1992] for the Nançay Decametric Array. The so-called "D_E effect" has generally been

[1] UMR 8639, Centre d'Études des Environnements Terrestre et Planétaires, Université de Versailles Saint-Quentin-en-Yvelines, Institut Pierre-Simon Laplace, CNRS, Vélizy, France.

[2] Space Research Institute, Austrian Academy of Sciences, Graz, Austria.

0148-0227/07/2006JA011911

interpreted in terms of a latitudinal dependence of the Jovian DAM radiation in angular width, in location, and in intensity.

1.3. Observation Frequency Conditions

[5] It is well known that the observation conditions, on ground, are modulated by the interference and ionosphere conditions, in particular late in the afternoon and in the evening (1700 UT to 2400 UT). Such observational conditions were discussed by several authors [*Genova et al.*, 1989, and references therein] who showed how the statistical occurrence is biased by the Earth's diurnal or annual rotation and by beats between these periods and the Jovian DAM emissions. The combination of ground-based and space observations allows us to cover a frequency range extending below the ionospheric cutoff. However, the CML-Io phase diagram of the Jovian decametric emissions seems also to be different when it is simultaneously observed from ground-based station and from space. Using the Nançay Decametric Array station and the WAVES experiment, *Aubier et al.* [2000] showed that, besides the ionospheric cutoff conditions, the receiver frequency range detects a very selective part of the Jovian DAM emissions. It appears that the area of the so-called Io-controlled occurrence zones decreases when the observation frequency increases. For example, the Io-controlled regions are clearly seen at high frequency, around 30 MHz, and are nearly absent at frequencies lower than 15 MHz [e.g., *Aubier et al.*, 2000, Figure 4].

[6] In the present paper, we investigate the location of the active longitude range on the theoretical CML-Io phase diagram, taking into consideration key parameters such as the observation frequency, the half-angle of the emission hollow cone, the lag of the active flux tube, and the Jovicentric declination of the Earth. Figure 1 displays these main parameters related to the radio emissions and the corresponding hollow cone.

2. Theoretical Outlines

[7] Like other nonthermal planetary radio emissions, the generation of the Jovian decametric radiation is attributed to the cyclotron maser instability (CMI), the theory of which was introduced by *Wu and Lee* [1979] (see the review by *Wu* [1985]). This mechanism is a resonant coupling between right-handed electromagnetic waves (relatively to the local magnetic field) and an electron population forming a magnetized plasma. The source of free energy needed by the CMI is contained in a positive gradient in perpendicular velocity $v_\perp$ of the electron distribution function f; that is, $\partial f/\partial v_\perp$ must be positive in certain domains of the momentum space [*Le Quéau et al.*, 1984a, 1984b; *Ladreiter*, 1991]. In our model, described in paper 1, we suppose that the electrons responsible for the radiation are accelerated in the neighborhood of Io's wake and follow an adiabatic motion along an active magnetic field line shifted by an angle δ relative to Io (see Figure 1). Some of these electrons disappear by collision in Jupiter's ionosphere; this phenomenon leads to a loss cone distribution function assumed to be the source of free energy needed by the CMI to produce the radiation. The waves are assumed to be emitted at the local gyrofrequency within a hollow cone of

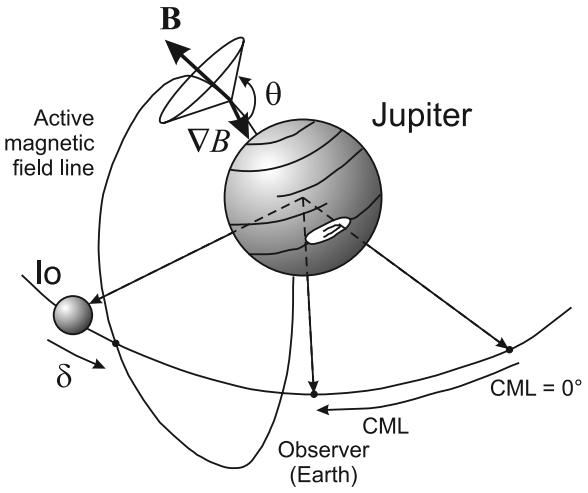

Figure 1. Schematic illustration of the parameters of our model. The radiation is assumed to be emitted at the local gyrofrequency along an active magnetic field line intersecting Io's wake with a lag δ. The radio emission is beamed into a hollow cone with half-angle θ and axis parallel to the direction of the gradient of the magnetic field modulus ∇B.

half-angle θ, the axis of which is parallel to the gradient of the local magnetic field modulus ∇B. We also make the significant assumption that, at Io, the electron distribution function is Maxwellian. Finally we compute the maximum growth rate of the waves produced by the CMI at all longitudes around Jupiter. All the details of the calculation are presented in paper 1.

[8] To sum up, the general dispersion equation for a right-handed mode is

$$k^2 - \frac{\omega^2}{c^2} - \frac{\mu_0 e^2}{4\pi m}\omega \iint \frac{\partial f/\partial v_\perp}{\omega - k_\parallel v_\parallel - \omega_c/\gamma}\, v_\perp^2\, dv_\perp\, dv_\parallel = 0. \quad (1)$$

Here $v_\perp$ and $v_\parallel$ are the components of the electron velocity perpendicular and parallel relative to the ambient magnetic field, $\mathbf{k}$ and ω are the wave number and the frequency of the wave, ω_c is the local gyrofrequency, γ the Lorentz factor, and m the electron mass. ω is a complex parameter, the imaginary part of which is the growth rate ω_i:

$$\omega = \omega_r + i\,\omega_i\,, \quad \omega \in \mathbf{C}\,, \quad \omega_r, \omega_i \in \mathbf{R}\,. \quad (2)$$

With the plasma frequency ω_p and the Dirac function $\delta()$, ω_i can be derived from equation (1):

$$\omega_i = \frac{\omega_p^2}{8}\int_0^{+\infty} v_\perp^2\, dv_\perp \int_{-\infty}^{+\infty} \frac{\partial f}{\partial v_\perp}\, \delta\left(\omega_r - k_\parallel v_\parallel - \frac{\omega_c}{\gamma}\right) dv_\parallel \quad (3)$$

with the condition

$$\iiint f(v_\parallel, v_\perp)\, d^3\mathbf{v} = 1\,. \quad (4)$$

The growth rate is significant when the resonance condition $\omega_r - k_\parallel v_\parallel - \omega_c/\gamma = 0$ in the integral of equation (3) is

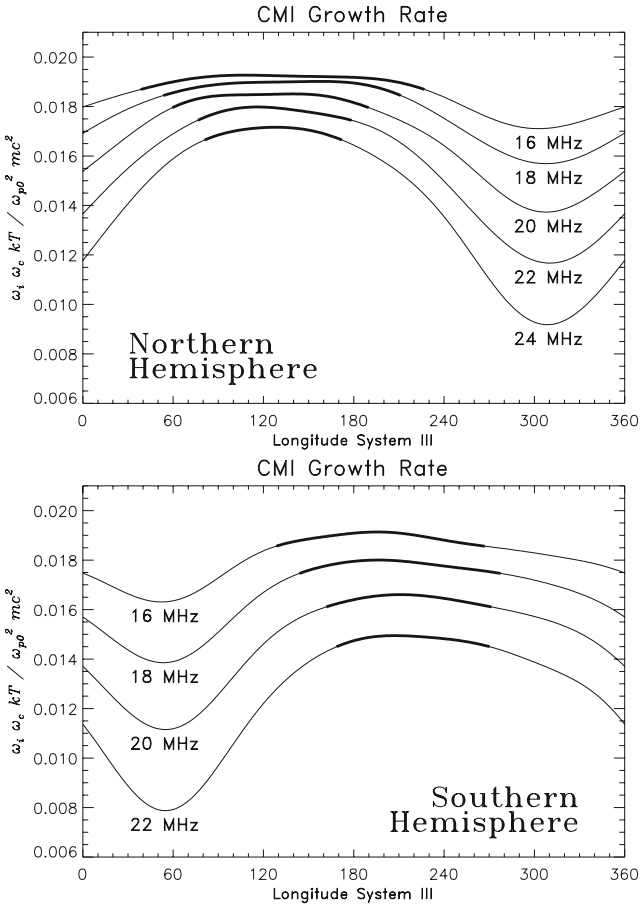

Figure 2. Dimensionless normalized growth rate of the cyclotron maser instability versus Jovian longitude (System III), calculated for both hemispheres for five frequencies: 16, 18, 20, 22, and 24 MHz. The growth rate ω_i is normalized to $\omega_{p0}^2\ mc^2/\omega_c\ kT$, where ω_{p0}^2 and T are the plasma frequency and the temperature of the initial electron distribution function at Io and ω_c is the local gyrofrequency. The thick parts of the curves define an active longitude range and correspond to a growth rate greater than 97% of the maximum rate.

fulfilled. In the phase space ($v_\parallel$, $v_\perp$), this condition can be approximated by a circle, the radius of which is

$$\Xi = c\left[\frac{k_\parallel^2 c^2}{\omega_c^2} + 2\left(1 - \frac{\omega_r}{\omega_c}\right)\right]^{1/2} \quad (5)$$

and the center of which is positioned at the point $v_\perp = 0$, $v_\parallel = v_0 = k_\parallel c^2/\omega_c^2$.

[9] The distribution function $f(s, \alpha, v)$, where α denotes the pitch angle and v the velocity, at any position s upon a magnetic field line carried away by Io and shifted in longitude by an angle δ, can be derived in the case of downgoing electrons toward Jupiter:

$$f_{\mathrm{down}}(s, \alpha, v) = \left(\frac{m}{2\pi kT}\right)^{3/2} e^{-mv^2/2kT}\ ; \quad (6)$$

here the pitch angle satisfies the condition $\pi/2 \le \alpha \le \pi$ for the northern hemisphere or $0 \le \alpha \le \pi/2$ for the southern hemisphere. We suppose that the electron distribution function in the vicinity of Io's wake is Maxwellian, characterized by a temperature T. A part of the upgoing electrons (toward Io), which have their mirror point in the Jovian ionosphere, has disappeared building a loss cone distribution function characterized by its open angle α_c. Let $\mathcal{P}(s, \alpha)$ be the probability of collision in the ionosphere for an upgoing electron as a function of the pitch angle α and the current abscissa s. A precise expression of $\mathcal{P}(s, \alpha)$ is given in paper 1, and $\mathcal{P}(s, \alpha) = 1$ for $0 \le \alpha \le \alpha_c$ (northern hemisphere) or $\pi - \alpha_c \le \alpha \le \pi$ (southern hemisphere). In the end, the distribution function for upgoing electrons is

$$f_{\mathrm{up}}(s, \alpha, v) = [1 - \mathcal{P}(s, \alpha)]\left(\frac{m}{2\pi kT}\right)^{3/2} \frac{e^{-mv^2/2kT}}{\cos^2\dfrac{\alpha_c}{2}} \quad (7)$$

with $\alpha_c \le \alpha \le \pi/2$ (north) or $\pi/2 \le \alpha \le \pi - \alpha_c$ (south). Everywhere else $f_{\mathrm{up}}(s, \alpha, v) = 0$.

[10] From equation (3), the maximum growth rate ω_i of the CMI can be derived as an integration along the resonance circle (v_0, Ξ). At a given frequency of emission $f = \omega/2\pi \simeq \omega_c/2\pi$, we numerically determine the position of the resonance circle (v_0, Ξ) for which the growth rate ω_i is positive and maximum. This calculation is done for each position of the active magnetic field line along which the radio emission is assumed to occur. In Figure 2, the maximum growth rate (actually a dimensionless normalized growth rate $\omega_i\ \omega_c\ kT/\omega_{p0}^2\ mc^2$, where ω_{p0} is the plasma frequency at Io) is plotted as a function of the Jovian longitude of this active magnetic field line. Several frequencies have been chosen: 16, 18, 20, and 22 MHz for both hemispheres, and also 24 MHz for the northern hemisphere. The maximum values of ω_i, implying a maximum efficiency for the CMI with regard to the DAM radiation, are found to be around 130° CML and 200° CML for the northern and southern hemispheres, respectively.

3. CML-Io Phase Diagram

[11] In a sense, the variation of the growth rate allows us to understand the efficiency of CMI as a function of the longitude of the active field line. Our model developed in paper 1 is founded on the hypothesis that the occurrence probability of the radiation is directly linked to the value of the growth rate ω_i. In this way, we define a zone of "active longitude" by the arbitrary criterion: $\omega_i \ge 0.97\ \max(\omega_i)$. This active zone is displayed for each frequency in Figure 2. The choice of the factor 0.97 leads to a good extent of these zones in longitude.

[12] In paper 1 we supposed that the radiation occurred in a hollow cone, the axis of which was aligned with the direction of the local magnetic field. In the present work we assume that the axis of this hollow cone is parallel to the gradient of the magnetic field modulus ∇B, and we define θ as the half-angle of the emission cone (measured from ∇B; see Figure 1). This choice is justified by the fact that the propagation of a wave, with frequency f, in the source medium is determined by the gradient of f_X, cutoff frequency of the X mode. Since the value of f_X is very near the local gyrofrequency, the waves amplified by the CMI emerge from a direction set by that of ∇B. As the vectors **B** and ∇B

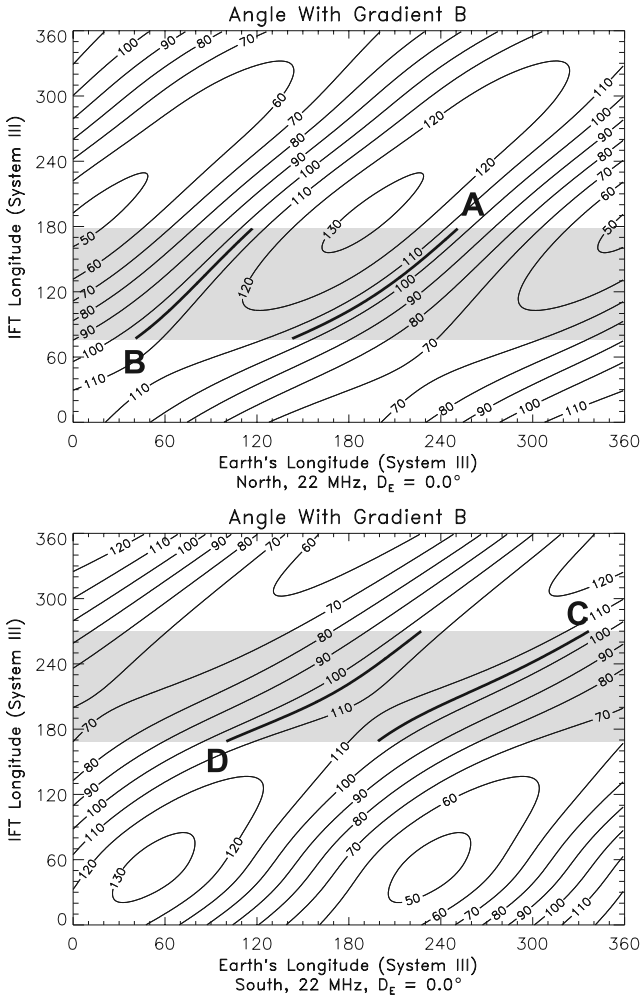

Figure 3. Contours of the angle between the gradient of the local magnetic field and the direction of the observer (located at the Earth) for a radiation at 22 MHz. An active longitude range is deduced from the curves in Figure 2 and are displayed in gray. The thick segments A, B, C, and D correspond to the intersection of an emission cone (with half-angle $\theta = 105°$) with the active longitude range. These segments are assumed to define the emissions with the highest occurrence probability.

are nearly aligned, the value of the angle θ is very close to that calculated in paper 1. Because of the propagation of the waves, $\theta \geq 90°$, two conditions are required for the radio emission to be observed from a given direction: (1) The active magnetic field line must cross the CMI active domain linked to Jupiter, and, at the same time, (2) the observer must be on the hollow cone associated with the beaming of the radiation. These two requirements are delimited by four segments (labeled A, B, C, D) in Figure 3, which displays the contours of the angle between the direction of the observer (supposed to be located at the Earth) and the gradient of the local magnetic field. The x and y axes correspond to the Jovicentric longitude of the Earth and of the active field line, respectively. The grey area represents the domain of active longitude, carried away by Jupiter, and deduced from the curves in Figure 2.

[13] In Figure 4, the four segments of high emission probability (A, B, C, D) are displayed in a usual CML-Io phase diagram in order to compare these theoretical areas with those whose occurrence is observed and is associated to the Io-controlled DAM emission (Io-A, Io-B, Io-C and Io-D). In our model, on the one hand, no refraction effect has been included; on the other hand, the northern sources Io-A and Io-B and southern sources Io-C and Io-D are considered to be right-hand and left-hand polarized, respectively. We do not take into consideration the double polarization sense observed for the Io-C source [see *Carr et al.*, 1983], a more complex model would be needed.

4. Parametric Study

[14] We analyze the variation of the source occurrence region for different values of the following parameters: the lead angle δ (0°, 20°, 40°), the half-angle θ of the hollow cone (100°, 105°, 110°), the emission frequency f (20, 22, 24 MHz), and the Jovicentric declination of the Earth D_E (−3°, 0°, +3°). Figure 5 displays the different CML-Io phase diagrams obtained for different sets of values given for (δ, θ, f, D_E).

4.1. Lead Angle δ

[15] The change of δ from 0° to 40° corresponds to an equal decrease of all sources in the Io phase while their longitudes remain unchanged. For instance the Io phase of source A decreases from 200° to 240° when the lead angle changes from 0° to 20°, respectively. In this case, one can note that the drifts in Io phase and lead angle are equal.

4.2. Declination of the Earth D_E

[16] The source regions are found to have two motions, one in Io phases and the other in longitudes. The pairs Io-A and Io-B and Io-C and Io-D shows differing motions when the Jovicentric declination of the Earth varies from −3° to +3°. For the first pair, longitudes of both sources are quasi-constant, but their Io phase increases and decreases for Io-A

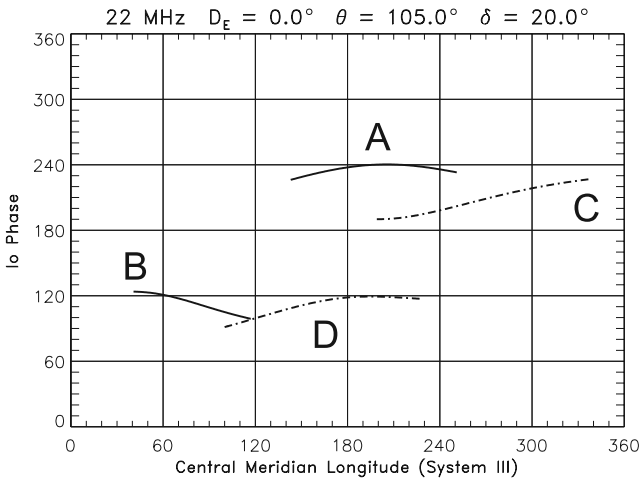

Figure 4. Curves of high occurrence probability versus central meridian longitude and the Io phase derived from Figure 3. Here the frequency is 22 MHz, the half-angle of the emission cone θ is 105°, the lead angle δ is 20°, and the declination of the Earth D_E is 0°.

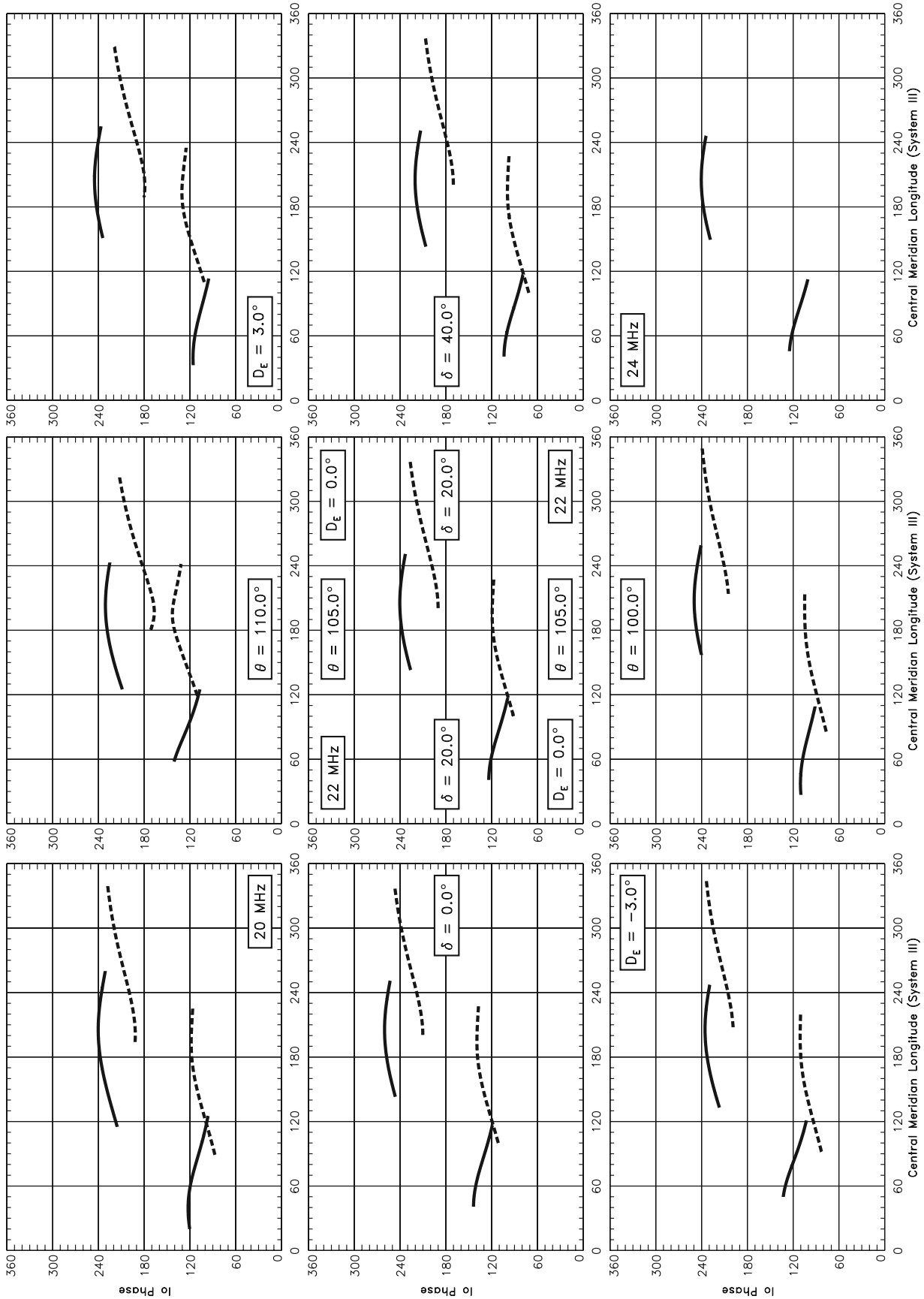
Io Phase
Central Meridian Longitude (System III)
20 MHz
θ = 110.0°
D_ε = 3.0°
22 MHz
δ = 0.0°
θ = 105.0°
δ = 20.0°
D_ε = 0.0°
24 MHz
θ = 100.0°
δ = 40.0°
D_ε = −3.0°

Figure 5

and Io-B, respectively. For the second pair, the main motion is the augmenting and diminishing of the Io phase of Io-D and Io-C sources. This means that the opening angle associated with the hollow cone of the Io-A and Io-B and Io-C and Io-D pairs increases and decreases, respectively, when the declination of the Earth changes from $-3°$ to $+3°$.

4.3. Half-Angle θ

[17] The half-angle θ is considered to vary from 100° to 110° for fixed values of the other parameters (f = 22 MHz, $\delta = 20°$, $D_E = 0°$). The parameter playing the most decisive role in the location of the sources is θ: the northern and southern hemisphere sources Io-A and Io-B and Io-C and Io-D are found to converge toward the central point of the CML-Io phase diagram when θ tends toward 110°.

4.4. Emission Frequency f

[18] As can be seen in Figure 2, the active longitude range is wider at low frequencies. As a consequence, the corresponding zones of high occurrence in the CML-Io phase diagram spread over a larger longitude range (e.g., 20 MHz in Figure 5). At 24 MHz the sources Io-C and Io-D have disappeared because they are assumed to emanate from the southern hemisphere where such a high frequency is rarely observed.

5. Discussion

[19] In the framework of the CMI theory, it is possible to give evidence of the existence of an active longitude, rotating with Jupiter, and favoring the radio decameter emissions. From the model developed by *Galopeau et al.* [2004], we have investigated the role of several parameters on the CML-Io phase diagram. In the following, we compare our main theoretical results with the conclusions deduced from other models and observations. Particular attention is given to the model assumptions, the D_E effect, and to the occurrence area dependence on the lead angle and the frequency.

5.1. Comparison With Other Theoretical Models

[20] In our study, the location of the active longitude (displayed in Figure 2) is mainly governed by the variation of ∇B at the footprint of the active magnetic field line (see Figure 1), whereas the electron distribution function is supposed to be constant at Io's orbit. Another model, proposed by *Zaitsev et al.* [2003, 2005], regards the origin of the active longitudes as caused by a change of the efficiency of the particle acceleration in Io's ionosphere and an electron scattering in the Io plasma torus. An interesting solution might lie in a combination of both models.

[21] Some of these parameters were studied in depth by *Imai et al.* [2002, and references therein] who proposed a model explaining the production of modulation lanes in Jupiter's dynamic spectra. Some effects are similar to the observations: it is notably the case for D_E and f. However, it is difficult to fit the four observed sources Io-A, Io-B, Io-C and Io-D simultaneously, especially Io-C and Io-D for which agreement is difficult in longitude. Moreover, our model allows only a right-hand polarization for the northern sources and a left-hand polarization for the southern ones.

5.2. Jovicentric Declination of the Earth

[22] Several studies investigated the variation of the DAM occurrence versus the D_E parameter [*Gulkis and Carr*, 1966; *Carr et al.*, 1970; *Conseil*, 1970; *Lecacheux*, 1974; *Thieman et al.*, 1975; *Barrow et al.*, 1982; *Boudjada and Leblanc*, 1992]. From our analysis, one can calculate the variation of the modelled source regions in the case of the Io-A, Io-B, and Io-C sources. It is possible to estimate for each source how the related curve (represented by two or three points) changes as a function of D_E. In the case of the Io-A curve, we consider three points: the beginning, the middle, and the end. For each point, we calculate the shift in CML and Io phase for the three values of the declination. All sources are found to have similar motions in Io phase; that is, the slope is usually negative when D_E increases. However, the Io-A source, as opposed to Io-B and Io-C, has a positive slope when D_E varies from $-3.0°$ to $+3.0°$. Two main results can be deduced from the D_E effect. First, the Io-B source region is shifted to lower values in the CML and Io phase. This change means that when D_E is about $+3.0°$, this source is observed earlier and the occurrence area is larger. The Jovian northern hemisphere, from which Io-B source is emitted, is inclined toward the direction of the Earth, and in this case the probability of Io-B occurrence is increased. The second result concerns the Io-A and the Io-C sources which are found to overlap when the declination attains high values and separate at low values. This action can be interpreted as the effect of the beams, coming from different hemispheres. Thus two separate sources are observed when $D_E \approx -3.0°$, the Io-A and the Io-C sources (with left-hand circular polarization) that come from northern and southern hemispheres, respectively. Both Io-A and Io-C sources (with right-hand circular polarization) overlap for $D_E \approx +3.0°$.

5.3. Hollow Cone and Lead Angle

[23] As mentioned above, the observed frequency corresponds to the local gyrofrequency related to the magnetic field of the planet. In an early study, *Genova and Aubier* [1985] compared the maximum observed frequency at the footprint of the Io flux tube (IFT) with the gyrofrequency given by the magnetic field model by *Acuña and Ness* [1976], which was deduced from the Pioneer magnetic measurements. The authors showed, for the first time, that the observed high-frequency limit was in disagreement with the value of the gyrofrequency. Moreover, the Io-controlled source field lines in the northern hemisphere needed to be shifted in longitude from the IFT by a lead angle estimated

Figure 5. Curves of high occurrence probability versus central meridian longitude and Io phase computed for several values of the lead angle δ (0°, 20°, and 40°), the half-angle of the emission hollow cone θ (100°, 105°, and 110°), the observation frequency f (20, 22, and 24 MHz), and the Jovicentric declination of the Earth D_E ($-3°$, 0°, and 3°). The central plot corresponds to a specific set of parameters ($\delta = 20°$, $\theta = 105°$, f = 22 MHz, and $D_E = 0°$); only the value of one parameter is changed in the other plots.

to ~40° at the surface of Jupiter, or else by up to 70° at Io's equatorial orbit, so that the high-frequency limit fits the gyrofrequency. In our study, we introduce the lead angle δ with the aim of investigating the source movement in the CML-Io phase diagram. We found that all Io-controlled sources have a decrease of their Io phase while their longitudes remain unchanged when the lead angle varies from 0° to 40°. This result is in concordance with those by *Genova and Aubier* [1985] for emissions radiated from the northern hemisphere in particular. One clearly sees in Figure 5 that the Io-A and the Io-B sources are in their correct locations when the lead angle is about 40°. Conversely, the emissions from the southern hemisphere, i.e., the Io-C and the Io-D sources, are in their correct positions (i.e., in CML-Io phase diagram) when only the lead angle is equal to zero. This result is also in agreement with those by *Genova and Aubier* [1985]. The concordance between the theoretical model and the Voyager observations validates the geometrical model which considers that Io-A and Io-C (Io-B and Io-D) belong to the east (west) edge of two hollow cones radiating from the northern and southern Jovian hemispheres.

5.4. Frequency Dependence of the Jovian DAM Occurrence

[24] The regular ground-based monitoring of the Jovian decametric emissions has allowed us to study the DAM occurrence at fixed frequencies and also at large frequency bandwidth [*Genova et al.*, 1989]. This occurrence is found to depend on the radio telescope sensitivity, the daily time coverage, the ionospheric cutoff, and the spectral time-frequency resolutions of the receiver. Thus the Voyager/PRA observations [*Warwick et al.*, 1977] permitted essentially avoiding the limited daily time coverage and ionospheric conditions. Space observations collected few months before and after each Voyager encounter with Jupiter allowed obtaining a synoptic view of the average statistical properties of the Jovian low-frequency radio emissions [*Alexander et al.*, 1981; *Barrow*, 1981; *Aubier and Genova*, 1985; *Genova and Aubier*, 1985, 1987]. From these studies, it is obvious that the area occurrence of the Io-controlled sources depends on the frequency. In Figure 3 of *Aubier and Genova* [1985] one can see that the emissions occur at all CML and Io phases, in particular for frequencies lower than 15 MHz where no distinction can be made between Io-controlled and non Io-controlled emissions. However, only very selective occurrence areas appear when the frequency increases from 15 MHz to more than 30 MHz. Such observations confirm our results concerning the variation of area occurrence versus the frequency. One should point out however that Galileo plasma wave data indicate that Io-controlled emissions can be distinguished in Io phase and CML at frequencies less than 15 MHz [*Kurth et al.*, 2000; *Hospodarsky et al.*, 2001; *Menietti et al.*, 1998]. According to our model the Io-controlled emissions associated to the southern hemisphere (i.e., Io-C and Io-D) disappear at frequencies higher than 24 MHz. The space observations did not provide a statistical study of the occurrence area against the polarization type of the emissions. However, ground-based observations, such as those performed at the Nançay Decametric Array [*Lecacheux*, 2000], measure the full Stokes parameters. *Boudjada and Genova* [1991] reported a statistical study of the left-hand polarized emissions considered as coming from the southern hemisphere. Those authors analyzed the spectral features and the occurrence of left-hand polarization events recorded for more than three years. According to this study, the maximum observed frequency of the Io-controlled emissions is not higher than 25 MHz. This upper frequency limit seems to be similar to those deduced from the modelled diagram.

6. Conclusion

[25] We proceed to a parametric study of the zones of high occurrence probability in the CML-Io phase diagram derived from the theoretical approach proposed by *Galopeau et al.* [2004], which gave evidence of the existence of a Jovian active longitude range favoring the decametric radio emission. For the present study, we principally consider four parameters that could be regarded as key factors: the lead angle of the active magnetic field line, the declination of the Earth, the half-angle of the emission cone, and the frequency of the radiation. The behavior of the theoretical CML-Io phase diagram, when those parameters vary, is fairly in agreement with the observed diagrams. In particular, we note that when the lead angle is equal to 40° (0°), the Io-A and Io-B (Io-C and Io-D) sources are localized in their correct occurrence regions as observed during the Voyager encounters of Jupiter. Also the absence of left-hand polarized emission at a frequency higher than 24 MHz is also predicted by this model, since those emissions are expected to emanate from the southern hemisphere. However, despite the agreement between the model and the observations, an important point must be mentioned. The model is not able to simultaneously fit the correct occurrence areas of the four Io-controlled sources at the same time. One needs to change a specific parameter to place the source to its observed position correctly, which is not satisfactory. This deficiency of the model seems to indicate that the active longitude (mainly linked to the magnetic field of Jupiter) is not the only factor determining the occurrence probability. The electron flux coming from Io could be another: the electron density and energy might depend on the longitude of the satellite, as proposed by *Zaitsev et al.* [2003]. A future study could be based on different distribution functions that change with the longitude of Io.

[26] **Acknowledgments.** Amitava Bhattacharjee thanks Michael Kaiser and John Menietti for their assistance in evaluating this paper.

References

Acuña, M. H., and N. F. Ness (1976), The main magnetic field of Jupiter, *J. Geophys. Res.*, *81*, 2917–2922.

Alexander, J. K., T. D. Carr, J. R. Thieman, J. J. Schauble, and A. C. Riddle (1981), Synoptic observations of Jupiter's radio emissions: Average statistical properties observed by Voyager, *J. Geophys. Res.*, *86*, 8529–8545.

Aubier, M. G., and F. Genova (1985), A catalogue of the high frequency limit of the Jovian decameter emission observed by Voyager, *Astron. Astrophys. Suppl. Ser.*, *61*, 341–351.

Aubier, A., M. Y. Boudjada, P. Moreau, P. H. M. Galopeau, A. Lecacheux, and H. O. Rucker (2000), Statistical studies of Jovian decameter emissions observed during the same period by Nancay Decameter Array (France) and WAVES experiment aboard Wind spacecraft, *Astron. Astrophys.*, *354*, 1101–1109.

Barrow, C. H. (1981), A catalogue of Jupiter's decametric emission observed by Voyager-1 and by Voyager-2 in the range 15–40 MHz, *Astron. Astrophys. Suppl. Ser.*, *46*, 111–114.

Barrow, C. H., A. Lecacheux, and Y. Leblanc (1982), Arc structures in the Jovian decametric emission observed from the Earth and from Voyager, *Astron. Astrophys.*, *106*, 94–97.

Bigg, E. K. (1964), Influence of the satellite Io on Jupiter's decametric emission, *Nature*, *203*, 1008–1011.

Boudjada, M. Y., and F. Genova (1991), The left-hand polarization sense of the Jovian decameter radiation, *Astron. Astrophys. Suppl. Ser.*, *91*, 453–467.

Boudjada, M. Y., and Y. Leblanc (1992), The variability of Jovian decametric radiation from 1978 to 1988, *Adv. Space Res.*, *12*(8), 95–98, doi:10.1016/0273-1177(92)90382-8.

Carr, T. D., A. G. Smith, F. F. Donivan, and H. I. Register (1970), Twelve-year periodicities in Jupiter's decametric radiation, *Bull. Am. Astron. Soc.*, *2*, 186.

Carr, T. D., M. D. Desch, and J. K. Alexander (1983), Phenomenology of magnetospheric radio emissions, in *Physics of the Jovian Magnetosphere*, edited by A. J. Dessler, pp. 226–284, Cambridge Univ. Press, New York.

Conseil, L. (1970), Contribution à l'étude du rayonnement de Jupiter sur ondes décamétriques, Ph.D. thesis, Paris Univ., Paris.

Galopeau, P. H. M., M. Y. Boudjada, and H. O. Rucker (2004), Evidence of Jovian active longitude: 1. Efficiency of cyclotron maser instability, *J. Geophys. Res.*, *109*, A12217, doi:10.1029/2004JA010459.

Genova, F., and M. G. Aubier (1985), Io-dependent sources of the Jovian decameter emission, *Astron. Astrophys.*, *150*, 139–150.

Genova, F., and M. G. Aubier (1987), High frequency limit and visibility of the non-Io and Io-dependent Jovian decameter radio emission, *Astron. Astrophys.*, *177*, 303–309.

Genova, F., P. Zarka, and A. Lecacheux (1989), Jupiter decametric radiation, in *Time Variable Phenomena in the Jovian System*, edited by M. J. S. Belton, R. A. West, and J. Rahe, NASA Spec. Publ., SP-494, 156-174.

Gulkis, S., and T. D. Carr (1966), Radio rotation period of Jupiter, *Science*, *154*, 257–259.

Hospodarsky, G. B., I. W. Christopher, J. D. Menietti, W. S. Kurth, D. A. Gurnett, T. F. Averkamp, J. B. Groene, and P. Zarka (2001), Control of Jovian radio emissions by the Galilean moons as observed by Cassini and Galileo, in *Planetary Radio Emissions V*, edited by H. O. Rucker, M. L. Kaiser, and Y. Leblanc, pp. 155–164, Austrian Acad. of Sci. Press, Vienna.

Imai, K., J. J. Riihimaa, F. Reyes, and T. D. Carr (2002), Measurement of Jupiter's decametric radio source parameters by the modulation lane method, *J. Geophys. Res.*, *107*(A6), 1081, doi:10.1029/2001JA007555.

Kurth, W. S., D. A. Gurnett, and J. D. Menietti (2000), The influence of the Galilean satellites on radio emissions from the Jovian system, in *Radio Astronomy at Long Wavelengths*, *Geophys. Monogr. Ser.*, vol. 119, edited by R. G. Stone et al., pp. 213–225, AGU, Washington, D. C.

Ladreiter, H. P. (1991), The cyclotron maser instability: Application to low-density magnetoplasmas, *Astrophys. J.*, *370*, 419–426.

Lecacheux, A. (1974), Periodic variations of the position of Jovian decameter sources in longitude (system III) and phase of Io, *Astron. Astrophys.*, *37*, 301–304.

Lecacheux, A. (2000), The Nançay Decameter Array: A useful step towards giant, new generation radio telescopes for long wavelength radio astronomy, in *Radio Astronomy at Long Wavelengths*, *Geophys. Monogr. Ser.*, vol. 119, edited by R. G. Stone et al., pp. 321–328, AGU, Washington, D. C.

Le Quéau, D., R. Pellat, and A. Roux (1984a), Direct generation of the auroral kilometric radiation by the maser synchrotron instability: An analytical approach, *Phys. Fluids*, *27*, 247–265.

Le Quéau, D., R. Pellat, and A. Roux (1984b), Direct generation of the auroral kilometric radiation by the maser synchrotron instability: Physical mechanism and parametric study, *J. Geophys. Res.*, *89*, 2831–2841.

Menietti, J. D., D. A. Gurnett, W. S. Kurth, J. B. Groene, and L. J. Granroth (1998), Galileo direction finding of Jovian radio emissions, *J. Geophys. Res.*, *103*, 20,001–20,010.

Thieman, J. R., A. G. Smith, and J. May (1975), Motion of Jupiter's decametric sources in Io phase, *Astrophys. Lett.*, *16*, 83–86.

Warwick, J. W., J. B. Pearce, R. G. Peltzer, and A. C. Riddle (1977), Planetary radio astronomy experiment for Voyager missions, *Space Sci. Rev.*, *21*, 309–327.

Wu, C. S. (1985), Kinetic cyclotron and synchrotron maser instabilities—Radio emission processes by direct amplification of radiation, *Space Sci. Rev.*, *41*, 215–298.

Wu, C. S., and L. C. Lee (1979), A theory of the terrestrial kilometric radiation, *Astrophys. J.*, *230*, 621–626.

Zaitsev, V. V., V. E. Shaposhnikov, and H. O. Rucker (2003), Electron acceleration in the ionosphere of Io, *Astron. Rep.*, *47*, 701–708.

Zaitsev, V. V., V. E. Shaposhnikov, and H. O. Rucker (2005), Electron acceleration at Io's ionosphere and origin of active longitudes in the Jovian decametric radio emission, *Adv. Space Res.*, *36*, 2106–2109, doi:10.1016/j.asr.2005.03.045.

M. Y. Boudjada and H. O. Rucker, Space Research Institute, Austrian Academy of Sciences, Schmiedlstraße 6, A-8042, Graz, Austria. (mohammed.boudjada@oeaw.ac.at)

P. H. M. Galopeau, UMR 8639, Centre d'Études des Environnements Terrestre et Planétaires, Université de Versailles Saint-Quentin-en-Yvelines, Institut Pierre-Simon Laplace, CNRS, 10–12 Avenue de l'Europe, F-78140 Vélizy, France. (patrick.galopeau@cetp.ipsl.fr)